

*Letter to the Editor***The molecular cloud core M 17-North: New ISOCAM observations***R. Klein¹, Th. Henning¹, and D. Cesarsky²¹ Astrophysical Institute and University Observatory (AIU), Schillergässchen 2-3, D-07745 Jena, Germany² Institut d'Astrophysique Spatiale, Bâtiment 121, Université de Paris-Sud, F-91405 Orsay Cedex, France

Received 8 January 1999 / Accepted 30 January 1999

Abstract. We present spectro-imaging data of the molecular cloud core M17-North. The data have been obtained with the ISOCAM camera on board of the Infrared Space Observatory (ISO) using the circular variable filters (CVF). The spectra have a spectral resolution of about 40. They are dominated by PAH emission bands. A band at $16.6\ \mu\text{m}$ is detected which is ascribed to the family of the PAH bands. Further, the PAH bands display clearly Lorentzian line profiles. The observations led to the detection of a new mid-infrared source with a very strongly rising continuum. The observed spatial distribution of fine structure line emission of neon and argon ions is a sign for an ionizing source in M 17-North.

Key words: stars: formation – ISM: clouds – ISM: individual objects: M 17-North – infrared: general

1. Introduction

The cloud core M 17-North was detected by bolometer array observations at the IRAM 30 m-telescope at a wavelength of 1.3 mm (Henning et al. 1998, hereafter HKL). It belongs to the giant molecular cloud complex M 17. It is located in the Sagittarius-Carina spiral arm at a recently determined distance of 1.3 kpc (Hanson et al. 1997). The cloud core M 17-North is located $10'$ north of the optically bright H II region M 17, the Omega nebula.

The detection of a compact core in the millimetre continuum (mm core) made the object an extremely interesting target for the study of star formation and the properties of the dust and molecule population in a cloud core. Therefore, M 17-North was observed with all four instruments of the Infrared Space Observatory (ISO). The spectrometers detected a strongly rising continuum starting at about $20\ \mu\text{m}$ superimposed with fine structure lines and the unidentified infrared bands (UIBs). First results from ISO spectroscopy and a comparison of ground-based near- and mid-infrared (NIR/MIR) data and the mm ob-

servations with the ISO data can be found in HKL. The UIBs were interpreted as emission from polycyclic aromatic hydrocarbon clusters (PAHs). In this letter we present the results of recent ISOCAM observations of M 17-North.

2. Observations

The data were obtained with ISOCAM (Cesarsky et al. 1996) on board of the ISO satellite (Kessler et al. 1996). We used this camera for spectro-imaging with the circular variable filters (CVF). A pointed observation towards the mm core at RA(2000): $18^{\text{h}}20^{\text{m}}32^{\text{s}}.7$, DEC(2000): $-16^{\circ}01'42''.6$ was carried out in March 1998. Within one hour the full long-wavelength section (LW) of the CVF was scanned covering the wavelength range between 5 and $17\ \mu\text{m}$ with a spectral resolution of about 40. The 32×32 detector array covered a field of $3' \times 3'$. One pixel's field of view (PFOV) is $6'' \times 6''$, which means that the point spread function of the telescope is under-sampled.

The data reduction was performed with the "CAM Interactive Analysis" software (CIA). The data for the missing column 24 was interpolated from the adjacent columns. We noticed a positional discrepancy of $12''$ between the ISOCAM images and our NIR images and shifted the ISOCAM data by that amount.

3. Analysis

The main features of M 17-North can be seen in Fig. 1. The image displays the map at 1.3 mm with the mm core in the centre. The contours show the ISOCAM image at $15.1\ \mu\text{m}$ representing the MIR continuum. The continuum emission at these two different wavelengths both outline the extent of the molecular cloud. However, the relative intensities are quite different. The ISOCAM image displays a previously unknown strong MIR source (M 17N-IRS 3). The bright mm core has no comparable counterpart in the MIR. The cross in Fig. 1 at the mm core indicates the position for the H_2O maser given by Jaffe et al. (1981) which was originally found by Cesarsky et al. (1978).

3.1. The sources

Four sources in the ISOCAM images have NIR counterparts. Their coordinates are compiled in Table 1 and marked in Fig. 3.

Send offprint requests to: rklein@astro.uni-jena.de

* Based on observations with ISO, an ESA project with instruments funded by ESA Member States (especially the PI countries: France, Germany, the Netherlands and the United Kingdom) with the participation of ISAS and NASA.

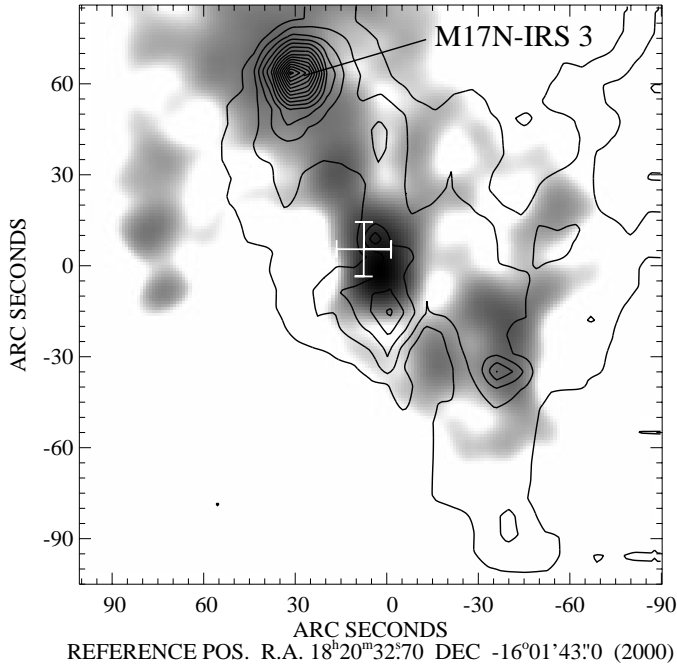


Fig. 1. ISOCAM image at $15.1 \mu\text{m}$ (contours: 0.4, 0.5, ... 1.9 Jy/pix) + mm continuum (logarithmic gray-scale). The cross shows the H_2O maser position.

Table 1. Coordinates of the infrared sources.

M 17 N-	RA(2000)	DEC(2000)	Comment
IRS 1	$18^{\text{h}}20^{\text{m}}32^{\text{s}}.8$	$-16^{\circ}01'33''$	at mm core
IRS 2	$18^{\text{h}}20^{\text{m}}33^{\text{s}}.0$	$-16^{\circ}01'48''$	at mm core
IRS 3	$18^{\text{h}}20^{\text{m}}34^{\text{s}}.6$	$-16^{\circ}00'40''$	disk cand.
IRS 4	$18^{\text{h}}20^{\text{m}}31^{\text{s}}.4$	$-16^{\circ}02'38''$	NIR star
IRS 5	$18^{\text{h}}20^{\text{m}}37^{\text{s}}.3$	$-16^{\circ}03'10''$	NIR star

One of these four sources is M 17 N-IRS 1. It was already mentioned together with M 17 N-IRS 2 in HKL. Both sources are located at the mm core and their NIR colour index is $m_{H-K'} > 1.7 \text{ mag}^1$. They are probably embedded in the mm core.

An outstanding source in the ISOCAM data is M 17 N-IRS 3. The most remarkable feature of this source is the strong rise of the MIR continuum (Fig. 2 bottom – right). A possible model for this continuum ($13\text{--}17 \mu\text{m}$) is $0.45 M_{\odot}$ of circumstellar matter at a temperature of 160 K. No cold dust is present in IRS 3 as there is no sign of the object in the mm continuum map. It has a K' -band brightness of $m_{K'}=11.9 \text{ mag}$ and a colour index $m_{H-K'}=1.15 \text{ mag}$. The reason for this moderately red $H-K'$ colour index, the surrounding warm dust, and no cold dust might be a warm disk seen face on.

¹ Due to an error in the data reduction the H -, and K' -band magnitudes given by HKL were too small by 1.08 mag and too large by 0.64 mag, respectively. Therefore, the stated colour index $m_{H-K'}$ was too small by 1.72 mag. The conclusions of our earlier paper are not affected by this mistake.

Table 2. Features in the ISOCAM spectra. Reliable estimates of the FWHM ($\Delta\lambda$) were possible only for the strong PAH bands.

$\lambda, \Delta\lambda$ in μm	PAH bands		others	
	λ	origin	wavel.	origin
5.3		C-H out-of-plane	7.0	[Ar II]
5.7		C-H out-of-plane	9.0	[Ar III]
6.261	0.15	C-C stretch	9.7	$\text{H}_2\text{S}(3)$
7.686	0.35	C-C stretch	10.5	[S IV]
8.567	0.19	C-H stretch	12.8	[Ne II] ¹
11.34	0.31	C-H out-of-plane bend	15.6	[Ne III]
13.6		C-H out-of-plane bend		
14.3		C-H out-of-plane bend		
16.6		ring deformation		

¹ blended with the PAH feature at $12.7 \mu\text{m}$

In the NIR the two objects M 17 N-IRS 4 and 5 appear as bright stars. The ISOCAM spectra of IRS 4 and 5 are the only spectra which are flat or declining to longer wavelengths (Fig. 2 lower-left panel), because of the stellar spectrum which is seen on the short wavelength side of the spectra.

3.2. The PAH bands

The first fact to mention is the dominance of the PAH emission in the ISOCAM spectra. In the wavelength range from 5 to $14 \mu\text{m}$, the contribution of the PAH bands to the observed flux is at least 50% and 70% on average. The emission in the PAH bands is more extended than the continuum radiation. From the edge of the molecular cloud to the north-west, the PAH emission is continuously rising. It is very strong in the north-western part of the observed field while the underlying continuum is relatively weak (cf. Fig. 3). A spectrum of this region is displayed in the upper right panel of Fig. 2.

Table 2 lists the detected features in the spectrum. Besides the known strong PAH bands and fine structure lines there is a new band at $16.6 \mu\text{m}$. This band was not detected in the spectrum obtained with ISO's short wavelength spectrometer (SWS) (HKL) as it is weak at the mm core. We ascribe it to the family of PAH bands because it seems to have a similar spatial distribution. The band is at the edge of the wavelength range and, therefore, it is difficult to estimate the band's height and width. A feature at $16.4 \mu\text{m}$ was already detected by Moutou et al. (1998) in NGC 7023 and was ascribed to large compact PAHs, possibly containing pentagons.

The PAH bands show Lorentzian line profiles. A fit of the bands with Gaussian profiles does not describe the data. As a consequence of the broad wings of the Lorentzian lines almost all flux in the fitted range belongs to the PAH bands. Only a weak continuum remains. The low spectral resolution of about 40 or the intrinsic line profile of the CVF are not the reasons for the observed Lorentzian line profiles. The PAH bands in the SWS spectra of M 17-North which have a resolution of about 200 are also better described with Lorentzian than with Gaus-

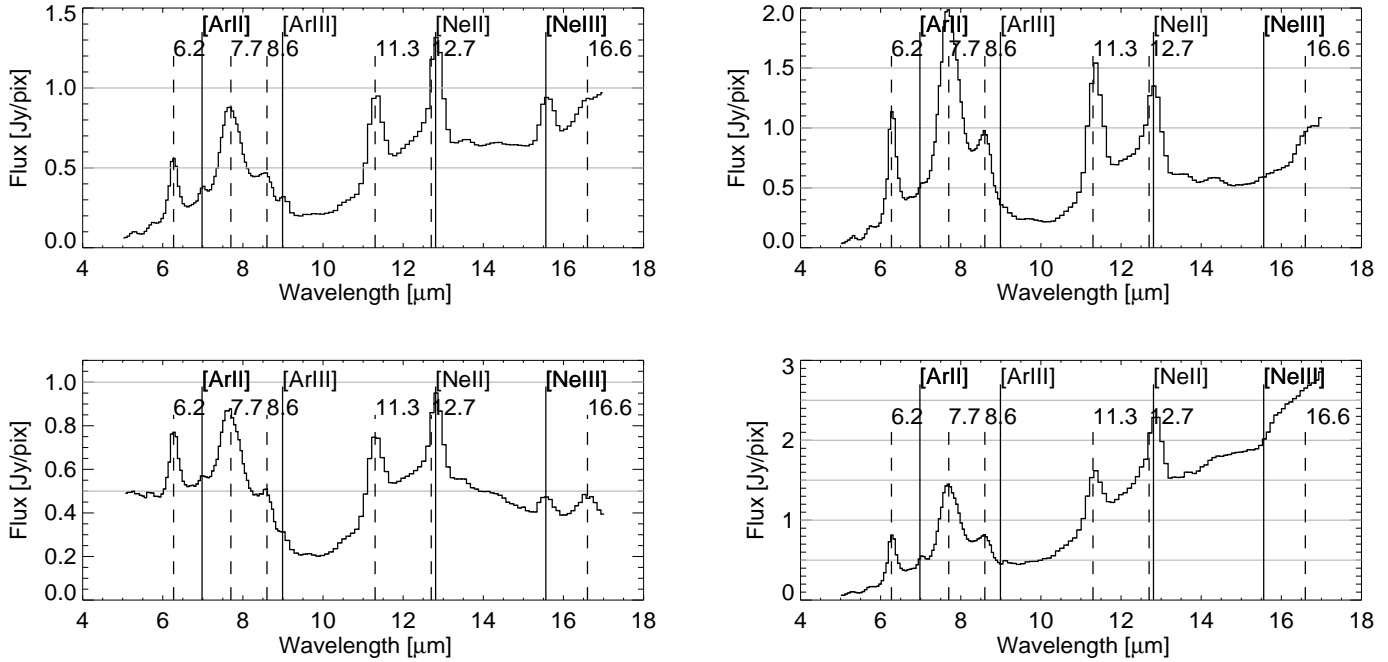


Fig. 2. Four CVF-spectra: *top left* – the mm core, *top right* – strong PAH emission in the NW, *bottom left* – IRS 5, *bottom right* – IRS 3. The vertical lines indicate the position of the main features (solid: PAH bands, dashed: fine structure lines). In order to make the different flux scales more apparent, every 0.5 Jy/pixel a horizontal line is drawn.

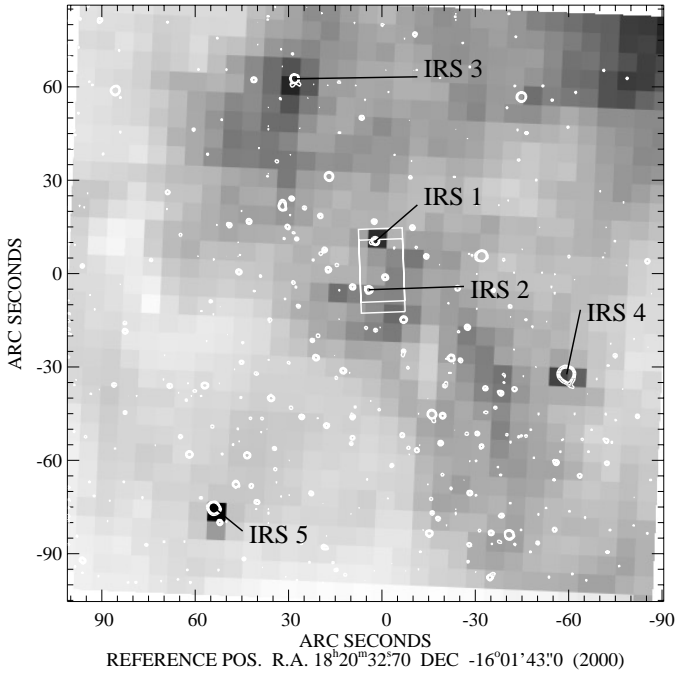


Fig. 3. ISOCAM at 6.6 μm + K'-band contours. The boxes mark the SWS apertures (cf. Sect. 3.2).

sian line profiles but the asymmetry of the bands in the SWS spectra is not reproduced. A full discussion of the analytical fit to ISOCAM spectra is done by Boulanger et al. (1998). They propose that the Lorentzian line profile is the result of the lifetime ($\tau \approx 10^{-13}$ s) of the emitting energy levels though this

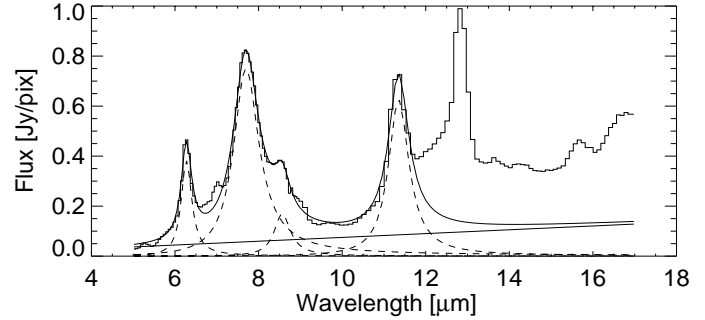


Fig. 4. Example for a fit of the PAH bands with Lorentzians. The histogram is the original spectrum. The smooth line is the sum of the low continuum (straight line) and the four Lorentzians (dashed lines).

leads to immense Einstein coefficients ($A \sim 1/\tau$) as pointed out by Siebenmorgen et al. (1998).

3.3. Fine structure lines

Only the lines of [Ar II] at 7.0 μm , [Ne III] at 15.6 μm , and [Ar III] at 9.0 μm (ordered by average in-band power) are suitable for an analysis of their spatial distribution. The regions which emit these fine structure lines are displayed in Fig. 5. The emission region of [Ar III] is similar to [Ne III]. Both lines are confined to an area around the mm core and the maser. The compact appearance of this region indicates the presence of an ionizing source somewhere near its centre. Regarding the total radio continuum flux from M 17-North (Wilson et al. 1979) one would expect an O9-star. The ionizing source cannot be deeply embedded in the mm core, because its ionizing radiation could

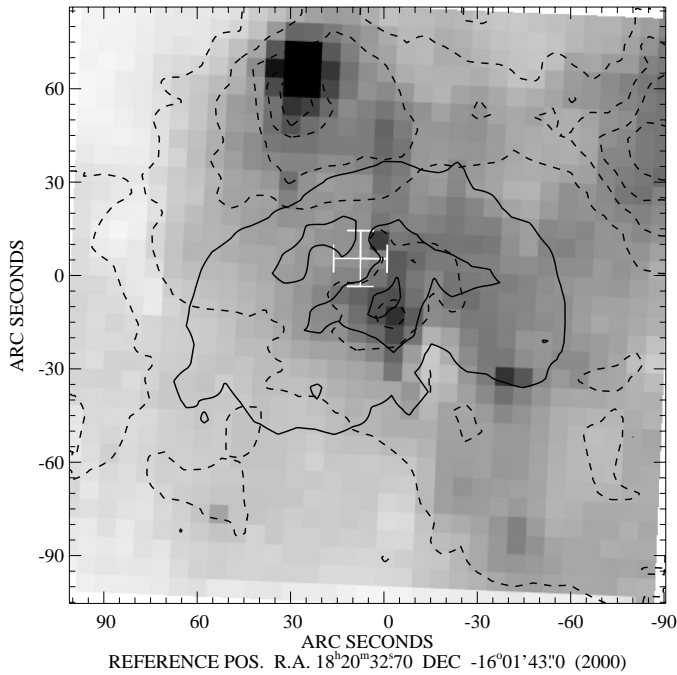


Fig. 5. ISOCAM at $15.1 \mu\text{m}$ (MIR continuum) and contours for $[\text{Ar II}]$ at $7.0 \mu\text{m}$ (dashed contour) and $[\text{Ne III}]$ at $15.6 \mu\text{m}$ (solid contour). The contours are spaced by $5 \cdot 10^{-7} \text{Wm}^{-2}\text{sr}^{-1}$.

not escape the core and ionize such a large region. It must be hidden behind the core. From a radiative transfer model (RTM) HKL derived a visual extinction of $A_V = 80$ mag from the centre of the mm core to the extended envelope. Calculations adopting the new distance to M 17 of 1.3 kpc changed this value to 70 mag. The core is responsible for 20 mag of extinction. An O9-star behind the mm core ($A_V \gtrsim 40$ mag) would have NIR H- and K-band magnitudes like IRS 1 ($m_H = 15.6$ mag, $m_K = 12.9$ mag). In this case the H II region is behind the mm core and the $[\text{Ne III}]$ radiation is extinguished by the core. According to the RTM, the extinction of the core is 0.8 mag at $15.5 \mu\text{m}$. In Fig. 5 this absorption (measured 0.6 mag) can be seen. There are two maxima and the mm core and the maser are located between them. Whether IRS 1 is an object embedded in the core or the ionizing source behind it or to which object the maser is associated has to be decided with further observations. Emission by $[\text{Ar II}]$ mainly originates from a bar north of the $[\text{Ne III}]$ emission region but is found everywhere where also mid-infrared continuum emission is detected. The $[\text{Ar II}]$ emission by the more easily ionized argon traces the interface where the ionizing radiation hits the cloud surrounding the core and the ionizing source behind it.

4. Summary

The main results of the ISOCAM observations of M 17-North are:

1. The coincidence of the MIR emission and the mm continuum emission region. The emission at both wavelengths traces the extent of the molecular cloud but the relative intensities differ in the two maps.
2. The detection of the source M 17 N-IRS 3. The detected circumstellar matter may form a disk seen face on.
3. The fit of the PAH bands with Lorentzian line profiles. The fact that the Lorentzian line profiles account for almost all flux in the PAH band region supports the PAH hypothesis.
4. The detection of a band at $16.6 \mu\text{m}$ which is ascribed to the family of PAH bands.
5. The compact region of emission of doubly ionized argon and neon, which indicates the presence of an O-type star in M 17-North.

Further investigations have to be done to reveal the nature of M 17 N-IRS 3 and -IRS 1 and to identify the ionizing source in M 17-North.

Acknowledgements. R. K. acknowledges support through the BMBF-Verbundforschung Astronomie/Astrophysik grant No. 50 OR 9414 9. The ISOCAM data presented in this paper were analyzed using “CIA”, a joint development by the ESA Astrophysics Division and the ISOCAM Consortium led by the ISOCAM PI, C. Cesarsky, Direction des Sciences de la Matière, C.E.A., France.

References

- Boulanger F., Boissel P., Cesarsky D., Ryter C., 1998, *A&A* 339, 194
 Cesarsky C. J., Abergel A., Agnès P., et al., 1996, *A&A* 315, L32, ISO special issue
 Cesarsky C. J., Cesarsky D. A., Churchwell E., Lequeux J., 1978, *A&A* 68, 33
 Hanson M. M., Howarth I. D., Conti P. S., 1997, *ApJ* 489, 698
 Henning Th., Klein R., Launhardt R., Lemke D., Pfau W., 1998, *A&A* 332, 1035, (HKL)
 Jaffe D. T., Güsten R., Downes D., 1981, *ApJ* 250, 621
 Kessler M. F., Steinz J. A., Anderegg M. E., et al., 1996, *A&A* 315, L27, ISO special issue
 Moutou C., Sellgren K., Léger A., et al., 1998, In: J. Yun and R. Liseau (eds.), Vol. 132 of *ASP Conference Series*, p. 47
 Siebenmorgen R., Natta A., Krügel E., Prusti T., 1998, *A&A* 339, 134
 Wilson T. L., Fazio G. G., Jaffe D., Kleinmann D., Wright E. L., Low F. J., 1979, *A&A* 76, 86